Utilizing the Drake Passage Time-series to understand variability and change in subpolar Southern Ocean pCO_2

Amanda R. Fay[1], Nicole S. Lovenduski[2], Galen A. McKinley[1], David R. Munro[2], Colm Sweeney[3-4], Alison R. Gray[5], Peter Landschützer[6], Britton B. Stephens[7], Taro Takahashi[1], Nancy Williams[8]

[1] Lamont Doherty Earth Observatory of Columbia University, New York, NY, USA
[2] Department of Atmospheric and Oceanic Sciences and Institute of Arctic and Alpine Research, University of Colorado, Boulder, CO, USA
[3] Cooperative Institutes for Research in Environmental Sciences, University of Colorado, Boulder, CO, USA
[4] NOAA Earth System Research Laboratory, Boulder, CO, USA
[5] School of Oceanography, University of Washington, Seattle, WA, USA
[6] Max Planck Institute for Meteorology, Hamburg, Germany
[7] National Center for Atmospheric Research (NCAR), Boulder, CO, USA
[8] College of Earth, Ocean, and Atmospheric Sciences, Oregon State University, Corvallis, OR, USA

Abstract

The Southern Ocean is highly under-sampled for the purpose of assessing total carbon uptake and its variability. Since this region dominates the mean global ocean sink for anthropogenic carbon, understanding temporal change is critical. Underway measurements of pCO_2 collected as part of the Drake Passage Time-series (DPT) program that began in 2002 inform our understanding of seasonally changing air-sea gradients in pCO_2, and by inference the carbon flux in this region. Here, we utilize available pCO_2 observations to evaluate how the seasonal cycle, interannual variability, and long-term trends in surface ocean pCO_2 in the Drake Passage region compare to that of the broader subpolar Southern Ocean. Our results indicate that the Drake Passage is representative of the broader region in both seasonality and long-term pCO_2 trends as evident through the agreement of timing and amplitude of seasonal cycles as well as trend magnitudes both seasonally and annually. The high temporal density of sampling by the DPT is critical to constraining estimates of the seasonal cycle of surface pCO_2 in this region, as winter data remain sparse in areas outside of the Drake Passage. An increase in winter data would aid in reduction of uncertainty levels. On average over the period 2002-2016, data show that carbon uptake has strengthened with annual surface ocean pCO_2 trends in the Drake Passage and the broader subpolar Southern Ocean less than the global atmospheric trend. Analysis of spatial correlation shows Drake Passage pCO_2 to be representative of pCO_2 and its variability up to several hundred kilometers away from the region. We also

compare DPT data from 2016 and 2017 to contemporaneous pCO_2 estimates from autonomous biogeochemical floats deployed as part of the Southern Ocean Carbon and Climate Observations and Modeling project (SOCCOM) so as to highlight the opportunity for evaluating data collected on autonomous observational platforms. Though SOCCOM floats sparsely sample the Drake Passage region for 2016-2017 compared to the Drake Passage Time-series, their pCO_2 estimates fall within the range of underway observations given the uncertainty on the estimates. Going forward, continuation of the Drake Passage Time-series will reduce uncertainties in Southern Ocean carbon uptake seasonality, variability, and trends, and provide an invaluable independent dataset for post-deployment assessment of sensors on autonomous floats. Together, these datasets will vastly increase our ability to monitor change in the ocean carbon sink.

1. Introduction

The Southern Ocean plays a disproportionately large role in the global carbon cycle. Over the past few decades, the ocean has absorbed approximately 26% of the carbon dioxide (CO_2) emissions from fossil fuel burning and land use change [Le Quéré et al., 2016, 2017], and since the preindustrial era, the ocean has been the primary sink for anthropogenic emissions [McKinley et al., 2017; Ciais et al., 2013]. The Southern Ocean (south of 30°S) accounts for almost half of the total oceanic sink of anthropogenic CO_2 [Frölicher et al., 2015; Gruber et al., 2009; Takahashi et al., 2009]. Though the importance of this region is widely understood, the relative scarcity of surface ocean carbon-related observations in the Southern Ocean hampers our ability to understand how this anthropogenic CO_2 uptake occurs against the background of natural variability.

Observations and models suggest large variability in the strength of Southern Ocean CO_2 uptake on decadal timescales. Several studies have reported a slow-down or reduction in the efficiency of Southern Ocean CO_2 uptake from the 1980's to the early 2000's [Le Quéré et al., 2007; Lovenduski et al., 2008; Metzl 2009; Takahashi et al., 2012; Fay and McKinley, 2013; Lovenduski et al., 2015; Landschützer et al., 2014a, 2015a], followed by a substantial strengthening of the Southern Ocean CO_2 sink since 2002 [Fay and McKinley, 2013; Fay et al., 2014; Landschützer et al., 2015a; Munro et al., 2015a; Xue et al., 2015].

Continued observational sampling efforts and coordination are required for quantifying and understanding decadal changes in this important CO_2 sink region.

Initiated in 2002 and continuing to present, the Drake Passage Time-series is unique among Southern Ocean research programs in both its spatial and temporal coverage. High-frequency underway observations of the surface ocean partial pressure of CO_2 (pCO_2) are collected on the Antarctic Research and Supply Vessel *Laurence M. Gould* on up to 20 crossings per year from the southern tip of South America to the Antarctic Peninsula, spanning the Antarctic Circumpolar Current (ACC) and its associated Antarctic Polar Front [Munro et al., 2015a, 2015b]. The DPT is also notable for sampling surface ocean pCO_2 during the austral winter in all years from 2002 to present, providing valuable information about the full seasonal cycle of pCO_2 in the poorly sampled Southern Ocean. Other ships have contributed observations in the Drake Passage region including the *Polarstern* and the *Nathaniel B. Palmer*, however none have the consistent temporal coverage as provided by the DPT.

The surface ocean pCO_2 observations from the DPT have provided the foundation for larger data sets, which have been extensively used to examine variability and trends in CO_2 uptake in the broader Southern Ocean [Fay and McKinley, 2013; Fay et al., 2014; Majkut et al., 2014; Landschützer et al., 2014b, 2015b; Rödenbeck et al., 2015, Gregor et al., 2018]. In many of these studies, interpolated estimates of Southern Ocean pCO_2 are used in conjunction with measurements of atmospheric pCO_2 to estimate variability and trends in the air-sea pCO_2 gradient and, when combined with wind speed, air-sea CO_2 fluxes.

The physical oceanography of the Drake Passage region is unique in the Southern Ocean. Here, the strong flow of the zonally unbounded ACC is funneled through a narrow constriction (~800 km), making it an ideal location for sampling across the entire ACC system over a relatively short distance [Sprintall et al., 2012]. At the same time, the unique nature of this circulation could potentially reduce the degree to which the Drake Passage region is representative of the broader subpolar region. The DPT program takes advantage of frequent *Gould* crossings to conduct physical and biogeochemical sampling of the ACC system. Thus, before conclusions can be drawn about large-scale Southern Ocean carbon uptake and its

variability using data from the DPT, it is important to document how pCO_2 in this particular region compares with pCO_2 measured elsewhere in the subpolar Southern Ocean. In this study, we utilize available ship-based surface ocean pCO_2 observations collected in the subpolar Southern Ocean to evaluate how the seasonal cycle, interannual variability, and long-term trends of surface ocean pCO_2 in the Drake Passage region compare to that of the broader subpolar Southern Ocean. Further, we highlight the opportunity for post deployment assessment of autonomous observational platforms passing through the Drake Passage utilizing the high frequency, underway pCO_2 measurements from the DPT.

2. Data

This study uses several observational datasets and data products of surface ocean pCO_2 in the Southern Ocean: measurements from the Surface Ocean CO_2 Atlas (SOCAT), which includes underway measurements from the DPT, interpolated estimates of the SOCAT data using a self-organizing map feed-forward neural network (SOM-FFN) approach, and calculated pCO_2 estimates from biogeochemical Argo floats. While the SOCAT database reports the fugacity of carbon dioxide (fCO_2), for our analysis we consider datasets reporting pCO_2 and fCO_2 to be interchangeable. This is an acceptable assumption for surface ocean observations as CO_2 behaves closely to an ideal gas. Globally, the difference between these parameters is less than 2 μatm, with fCO_2 being smaller than pCO_2 by no more than 2 μatm due to temperature dependence. This is roughly the reported uncertainty of shipboard observations of pCO_2 and well within the uncertainty of the observation-based pCO_2 estimates. Below, we describe each of these data sources in turn.

2.1 The Drake Passage Time-series (DPT)

A unique dataset of ongoing year-round observations beginning in 2002 is available from the Drake Passage Time-series. This data set provides an unprecedented opportunity to characterize the mean and time-varying state of the Drake Passage and surrounding waters using direct observations. In addition to high frequency underway observations of surface ocean pCO_2, other physical and biogeochemical variables measured onboard allow for a complete understanding of the carbonate system in the Drake Passage.

Analytical methods used to measure pCO_2 to ±2 µatm are described in detail by Munro et al. [2015a, 2015b].

2.2 Surface Ocean CO_2 Atlas (SOCAT)

SOCAT is a global surface ocean carbon dataset of fCO_2 values (pCO_2 corrected for the non-ideal behavior of CO_2) [Sabine et al., 2013; Pfeil et al., 2013]. In this study, we utilize version 5 of this product (SOCATv5) and include data with a reported WOCE flag of 2 and cruise flags A-D which results in a dataset of roughly 18.5 million observations globally, spanning years 1957-2016, with uncertainties of ±2-5 µatm [Bakker et al., 2016]. This dataset includes over 740,000 observations contributed from the DPT. Despite the large number of observations available in the Southern Ocean, data is spatially and temporally concentrated, with strong seasonal biases. Most data are collected during reoccupations of supply routes to Antarctic bases or on repeat hydrographic lines, which leaves large bands of the Southern Ocean completely unsampled [Bakker et al., 2016].

2.3 Self-Organizing Map Feed-forward Network Product (SOM-FFN)

Landschützer et al., [2014b] use a two-step neural network approach to extrapolate the monthly gridded SOCAT product in space and time. This results in reconstructed, basin-wide monthly maps of the sea surface pCO_2 at a resolution of 1° × 1° [Landschützer et al., 2017]. Air–sea CO_2 flux maps are then computed using a standard gas exchange parameterization and high-resolution wind speeds. The neural network estimate is described and substantially validated in past publications [Landschützer et al., 2014, 2015a, 2016] and it was shown that the estimates fit observed pCO_2 data in the Southern Ocean with a root mean square error (RMSE) of about 20 µatm and with almost no bias [Landschützer et al., 2015a, supplementary material].

The SOM-FFN product used in this analysis was created from SOCATv5. Additionally, we generated an alternative SOM-FFN product (SOM-FFN-noDP) using the same methodological setup but excluding the pCO_2 data collected in the Drake Passage region for years 2002-2016, which represents the years of the DPT program.

2.4 SOCCOM Floats

The Southern Ocean Carbon and Climate Observations and Modeling (SOCCOM) project (http://soccom.princeton.edu) aims to deploy approximately 200 biogeochemical profiling floats over a five-year period (2015 to 2020) in an effort to fill observational gaps in the Southern Ocean. In total, over 100 floats carrying some combination of additional biogeochemical sensors (i.e., pH, nitrate, oxygen, fluorescence, and backscattering) have been collecting data since April 2014 [Johnson et al., 2017]. With the float's capability to measure pH and utilization of existing algorithms for predicting total alkalinity, pCO_2 can be calculated from the collected observations and compared to underway observations [Williams et al., 2017].

The uncertainty range for these calculated pCO_2 values is estimated to be 2.7% (±11 μatm at 400 μatm) and takes into account multiple sources of uncertainty including measurement error, uncertainties introduced through the quality control procedures, and uncertainties in seawater carbonate system thermodynamics [Williams et al., 2017]. pCO_2 estimates from profiling floats have not been included in the SOCAT database because they do not directly measure surface water CO_2. For consistency, we maintain this separation in our analysis and limit our study of SOCCOM floats to direct comparisons to DPT values in Section 5.

3. Methods

The SOCATv5 database from 2002-2016 is considered here to match the years of overlap with DPT observations, which began in 2002. The SOCAT dataset is then subsampled to include only observations with reported salinity values in the 33.5 - 34.5 range and a distance-to-land value greater or equal to 50 km. This step restricts our analysis to open-ocean observations, since coastal observations report lower salinity values, which correspond to low pCO_2 values due to the influence of fresh water and ice melt. SOCCOM float files were downloaded on 02 April 2018 and reported pCO_2 values, are an average of all data collected in the top 20m of water, calculated using alkalinity derived from the LIAR algorithm [Carter et al., 2016], to remain consistent with previous SOCCOM float analysis.

The Southern Ocean region of interest is the Southern Ocean Subpolar Seasonally Stratified (SPSS) biome as defined in Fay and McKinley [2014] as the region of the Southern Hemisphere with climatological SST <8^{o}C but excluding areas with a sea-ice fraction greater than or equal to 50% (Figure 1). While the SPSS biome encompasses the Drake Passage, we further define a Drake Passage region as the portion of the Southern Ocean SPSS biome bounded by 55^{o}W and 70^{o}W lines of longitude (Figure 1, black box). This is similar to the region analyzed in Munro et al [2015a] however it extends the region of interest to the northern and southern extents of the SPSS biome.

In order to compare the seasonal cycle and long-term trends in the Drake Passage with the broader SPSS biome, we analyze surface ocean pCO_2 from 3 subsets of the SOCAT database: SOCAT-all which includes all available SOCATv5 data from 2002-2016 in the SPSS biome, SOCAT-DP which includes SOCATv5 data within the longitudinally-defined Drake Passage region (Figure 1, with 62% of this data obtained by the LDEO/Univ. Colorado group), and SOCAT-noDP which excludes any data within the longitudinally-defined Drake Passage region of the SPSS biome. All datasets are first averaged to monthly, 1^{o}x1^{o} resolution. Monthly means are then calculated for the SPSS biome by first removing the background mean annual climatological value of pCO_2 at each 1^{o} x 1^{o} location [Landschützer et al., 2014a] to aid in accounting for the potential of spatial aliasing in the sparsely sampled Southern Ocean [Fay and McKinley, 2013].

Alternate definitions of the larger Southern Ocean region of interest were considered during our analysis, including a subdivision of the SPSS into a Northern SPSS and Southern SPSS, with the boundary defined by the location of the mean position in the Antarctic Polar Front [Freeman and Lovenduski 2016; Freeman et al., 2016; Munro et al., 2015b]. As discussed in Munro et al., [2015a], Drake Passage Time-series observations north of the front report higher pCO_2 values than to the south and they find a larger trend in pCO_2 in the north for years 2002-2015. Additionally, the seasonal cycle amplitude north of the front is much larger and well defined than south of the front. We see these patterns in the SOCAT dataset as well; however, given the goal of this research, we choose to consider the entire north-to-south extent of the SPSS

as a whole. Outside of the Drake Passage region, available data is limited such that analysis over north and south subregions would be impossible.

Additionally, we consider analysis over the Polar Antarctic Zone (PAZ), defined as the area between the Subantarctic Front and the sea ice zone [Williams et al., 2017] (Supplementary Figure 1). While differences exist in trends and seasonality when using the PAZ definition (Supplementary Figures 2-3), the overall conclusions of the relationship between SOCAT-DP and SOCAT-all remain largely unchanged when using this alternate regional definition.

Biome-scale monthly means are compared and used to calculate seasonal cycles and trends. Seasonal cycles are calculated by first removing a 1.95 μatm yr^{-1} trend to account for increasing atmospheric CO_2 during the 2002-2015 period [Dlugokencky et al., 2015]. Seasonal uncertainties (Figure 2) are estimated as 1 standard error from the mean of all available biome mean values for a given month. This is a conservative estimate of the uncertainty in any given month because of inconsistent annual coverage and spatial undersampling biases. Reported trends are calculated by fitting a single harmonic and linear trend to the biome-scale monthly means as done in Fay and McKinley [2013]. Trends are not statistically different if the calculated mean seasonal cycle is removed instead of the choice to fit a harmonic to the data. Seasonal trends are calculated with a simple linear fit to the seasonal monthly means.

4. Results and Discussion

4.1 Seasonal cycle

The mean seasonal cycle of pCO_2 (corrected to reference year 2002) in the Southern Ocean SPSS biome for the 3 SOCAT datasets and the full SOM-FFN estimate indicate broad agreement (Figure 2). Here, surface ocean pCO_2 levels reach a maximum in austral winter (June to August), when deep mixing delivers carbon-rich water to the surface, and a minimum in austral summer (December to February), when biological production draws down the inorganic carbon from the surface [Takahashi et al., 2009]. Temperature also plays a role in modulating the pCO_2 seasonal cycle in the Southern Ocean. Winter cooling drives pCO_2 lower at the same time as deep winter mixing elevates surface carbon levels. During the summer, warming

temperatures raise pCO_2 while biological utilization of carbon drives surface pCO_2 levels lower [Munro et al., 2015b].

The average amplitude of the detrended seasonal cycle of pCO_2 (max-min) is 23 μatm (Figure 2), smaller than the high latitude oceans in the Northern Hemisphere [Takahashi et al., 2002, 2009; Landschützer et al., 2015b]. The small amplitude of the pCO_2 seasonal cycle in this region is due to the similar magnitude and opposite phasing of temperature and carbon supply/utilization effects [Munro et al., 2015b]. In all months, mean surface ocean pCO_2 levels in the Southern Ocean SPSS are below atmospheric which ranges from a global annual mean of 372 ppmv in 2002 to 399 ppmv in 2015, indicating that this region has been a persistent CO_2 sink over the period of analysis [Dlugokencky & Tans, 2017].

Figure 2 also shows the uncertainty of the seasonal mean, with shading representing 1 standard error from the monthly mean for each dataset, defined as the standard deviation divided by the square root of the sample size (here, number of years with available data in that month). Uncertainty estimates vary for each month of the seasonal cycle with a minimum uncertainty of 1.1 μatm (June, SOCAT-DP) to a maximum of 5 μatm (July, SOCAT-DP). These estimates are of the same magnitude as the measurement accuracy of underway pCO_2 in SOCAT (±2-5 μatm).

Figure 3 indicates how diverse Southern Ocean pCO_2 data density is in space and time. Compared to the regular sampling of the DPT, there are many fewer repeated occupations of SR03 south of Australia [Shadwick et al., 2015], along the Prime Meridian [Hoppema et al., 2009; Van Heuven et al., 2011], and in the southwestern Indian sector [Metzl et al., 1999; Lo Monaco et al., 2005, 2010; Metzl, 2009]. Specifically, during austral winter, data availability outside of the Drake Passage region is extremely limited due to the few ships operating in winter and the difficult conditions that the wintertime Southern Ocean presents to data collection efforts (Figure 3b).

Despite irregular sampling, average seasonal cycles of the 3 SOCAT datasets are quite similar, with few statistically significant differences given the uncertainty bounds. SOCAT data from the Drake Passage

region (SOCAT-DP, gray) exhibits relatively large estimated uncertainty (average for all months = 2.22 μatm), despite the frequent coverage and smaller region considered. This indicates that large interannual variability is inherent to the Drake Passage region, especially in the well-observed austral summer months. Despite data being much more regularly collected in this region than in the rest of the Southern Ocean (Figure 3), there are still months of quite limited observations, specifically July and August (Figure 2). SOCAT-all has monthly uncertainties averaging 1.7 μatm with the largest uncertainties in January and July (Figure 2, blue). Data availability for SOCAT-all is consistent for much of the year, with most months having observations in at least 13 of the 15 years considered in this analysis (Figure 2). The exceptions are July and August that have data from only 8 and 10 years, respectively.

The SOCAT-noDP seasonal cycle is similar to that of the other datasets but deviates in the austral fall/winter, specifically May and June. In winter, SOCAT-noDP suggests higher pCO_2 than SOCAT-DP or SOCAT-all, though the limited data in June and July must be considered when drawing conclusions from this difference (Figure 2, 3b). With June and July data available for fewer than 5 of the 15 years covered in the analysis it is possible that the peak shown here could be biased by the few years included, specifically for the month of June. In contrast, SOCAT-DP has data for nearly all of the years considered in these months. The data that is available during May and June in SOCAT-noDP is from regions downstream of the Drake Passage (Figure 3b).

Seasonal cycles are consistent when analyzing the PAZ region (Supplementary Figure 2), however the SOCAT-DP seasonal cycle exhibits two maxima possibly due to the omission of the southern area of the Drake Passage (Supplementary Figure 1) which would cause values for the PAZ region to be greater than those shown for the DP region of the SPSS. The June peak in SOCAT-noDP also remains when considering the PAZ region. Amplitudes are comparable given the uncertainty, however the seasonal amplitude for each dataset is slightly larger over the SPSS biome than the PAZ, likely due to the more northern expansion of the PAZ region downstream of the Drake Passage and the exclusion of the southern Drake Passage region in the boundary of the PAZ.

Overall, given available data, the seasonal cycles are statistically indistinguishable for data collected inside and outside of the Drake Passage region, for all months with at least 5 years of observations (Figure 2). This analysis of SOCAT pCO_2 data indicates that the Drake Passage seasonal cycle is representative of the broader SPSS biome seasonality, based on the available observations to date, but increased observations outside of the Drake Passage during May and June are needed to provide a more robust comparison. Additionally, the seasonal cycles from all 3 SOCAT datasets closely resemble the smoothed seasonality of the interpolated SOM-FFN product in the SPSS biome (Figure 2). Sparse sampling outside of the Drake Passage during winter months leads to this estimated seasonal cycle of SOCAT-all being driven by Drake Passage data. Enhanced wintertime data collection, especially in regions outside of the Drake Passage, is required to better constrain the full seasonal cycle of surface ocean pCO_2 in the Southern Ocean SPSS.

4.2 Interannual variability

The high resolution of the time-series data in the Drake Passage allows for close examination of temporal variability in pCO_2 with relatively low uncertainty [Munro et al., 2015a]. We investigate the interannual variability in Drake Passage pCO_2 in Fig. 4a, where deseasonalized and detrended anomalies [Fay and McKinley, 2013] from the SOCAT-DP dataset are shown in gray, with the black line representing these anomalies smoothed with a 12-month running mean. Over the 2002-2016 period, the variance in pCO_2 anomalies is 66 μatm^2. Monthly anomalies are as large as ±30 μatm, and 12-month smoothed anomalies as large as ±12 μatm in this dataset.

A model-based study by Lovenduski et al., [2015] finds interannual variability in pCO_2 to be low in the Drake Passage compared to other Southern Ocean regions for years 1981-2007. In contrast, we find that detrended and deseasonalized anomalies from SOCAT-noDP and SOCAT-DP have comparable variances (59 μatm^2 and 66 μatm^2). This result, however, is likely strongly affected by the previously discussed seasonal data gaps outside of the DP region or potentially by the different years considered in these two analyses. Conducting a similar analysis of the reported SOCAT sea surface temperature (SST) values does find the variance for SOCAT-DP to be significantly lower than SOCAT-noDP (0.93°C^2 and 2.72°C^2 respectively). As the same sampling issues exist for SST as for pCO_2 in SOCAT, an alternate method to

address this issue is needed to resolve these conflicting results.

The SOM-FFN data product offers complete seasonal and regional coverage, and thus the comparison of variance in Drake Passage to all the Southern Ocean can be made in this context. Results for SOM-FFN are different from both the SOCAT findings above and the results of Lovenduski et al., [2015]. For the SPSS biome area of SOM-FFN pCO_2, the variance of detrended and deseasonalized anomalies is significantly higher within the Drake Passage region than outside of the region (14.2 μatm^2 and 6.2 μatm^2, respectively). It should be noted that variances are significantly lower for the SOM-FFN because of its interpolation. We are left without a clear picture as to whether Drake Passage is more or less variable in pCO_2 than the rest of the Southern Ocean SPSS. This conundrum is clearly due to the lack of data availability, particularly outside the Drake Passage during winter months (Figure 3b).

Given the lack of data, the degree to which the Drake Passage represents interannual variability within the Southern Ocean SPSS can only be considered in the context of the SOM-FFN data product. To produce independent estimates of correlations between Drake Passage and other points, we use a version of the SOM-FFN product created without the inclusion of any observations in our defined Drake Passage region (SOM-FFN-noDP, Figure 4b), and assess correlations to SOCAT data within the Drake Passage. Anomalies have been detrended and deseasonalized, and grayed areas indicate that the correlation is not significant at the 95% confidence level (Figure 4b). The strongest positive correlations are within Drake Passage, upstream of the Drake Passage into the central Pacific SPSS, and in the Indian Ocean sector of the SPSS biome (Figure 4b). Weaker positive correlations are found in the western Pacific SPSS, as well as a few areas in the Atlantic sector of the SPSS. No regions of widespread strong negative correlations are observed in the SPSS biome. This is consistent with the analysis of Munro et al., [2015b] who estimate the footprint of the Drake Passage extending upstream into the eastern Pacific sector of the ACC.

4.3 Trends, 2002-2016

Trends for all data (annual), as well as summer (DJF) and winter (JJA), are estimated from the three SOCAT datasets, the SOM-FFN data product, and the SOM-FFN product subsampled as SOCAT-DP

(SOM-FFN-sampled), in all cases following the approach of Fay & McKinley [2013]. Similar to the climatological pCO_2 seasonal cycle, annual trends for the 3 SOCAT datasets are indistinguishable given the 68% confidence intervals (Figure 5, Supplementary Table 1).

All annual trends are less than the 2002-2016 atmospheric pCO_2 trend of 1.95 μatm yr^{-1} [Dlugokencky et al., 2015], indicating that the Southern Ocean has been a growing sink for atmospheric carbon over 2002-2016 (Figure 5, far left). Comparing the different estimates, SOCAT-DP (gray bar) and SOCAT-all (blue bar) have annual trends slightly below that of the full SOM-FFN, however with greater uncertainty bounds. The annual trend from the SOCAT-all dataset (blue) is nearly identical to the SOCAT-DP trend in both mean and uncertainty. These are not statistically different from the SOCAT-noDP, although the SOCAT-noDP dataset does yield a slightly larger annual trend. While SOCAT-noDP yields the largest annual trend of the 3 datasets, it still falls well below the atmospheric trend. These trends are comparable to those reported in Munro et al., [2015b], Takahashi et al., [2012], and Fay et al., [2014] despite these studies utilizing different datasets, methods, and regional boundaries. Takahashi et al., [2014], similar to Munro et al., [2015b], show that trends in the northern portion of the Drake Passage are greater than those south of the front. Our analysis of regions north and south of the front confirms this (not shown).

Sampling the SOM-FFN data product as the SOCAT-DP dataset (SOM-FFN-sampled) is one way to estimate the impact of the available data coverage in the Drake Passage region as compared to the hypothetical situation of perfect data coverage in the SPSS biome. Sampling lowers the trend, making it significantly smaller than the full SOM-FFN trend. This reduction leads to an annual trend very similar to that of SOCAT-DP and SOCAT-all. This conclusion emphasizes the need for increased observations around the Southern Ocean as it implies we are potentially not accurately capturing the true trend in this region with the available data coverage.

Conclusions of these comparisons are largely maintained for summer and winter trends (Figure 5, center and right). Uncertainty increases when considering seasonal trends due to reduced data quantity. All trends are statistically indistinguishable for summer months; however, the SOCAT-DP trend shows the largest

change from the reported annual trends. For winter, SOCAT-noDP is not shown because unlike SOCAT-all and SOCAT-DP, not all years have available data during this season (Figure 2). Overall, winter trends are slightly higher than summer trends. Even given the uncertainties, winter and summer trends are clearly distinguishable for SOCAT-DP, SOCAT-all, and the full and sampled SOM-FFN product. In each of these datasets, the winter trend is roughly 0.5 μatm yr^{-1} higher than the summer trend. While winter trends have larger differences and larger uncertainties, consistent with reduced data availability, this seasonal difference in trends is significant. Further and more detailed consideration of this seasonal comparison is warranted. Initial investigations indicate that 2016 had anomalously high wintertime pCO_2 values (not shown). Specifically when trends are calculated with the same datasets for 2002-2015, winter trends are significantly lower than the atmospheric trend (SOCAT-DP: 1.53±0.32 μatm yr^{-1}, SOCAT-all: 1.59±0.27 μatm yr^{-1}, SOM-FFN: 1.70±0.09 μatm yr^{-1}). It is important to consider the impact of anomalous values at the end of selected time-series, specifically for time-series less than 15 years [Fay & McKinley, 2013].

An investigation of trends from the full SOM-FFN product and that of the SOM-FFN-noDP product for the entire Southern Ocean SPSS biome for years 2002-2016 indicates an increasing carbon uptake by the ocean with some interannual variability (Figure 6). If the Drake Passage data is omitted during the creation of the product (SOM-FFN-noDP), carbon flux and pCO_2 trends are unchanged (Figure 6). Both estimates illustrate that for 2002-2016, the Southern Ocean SPSS biome was an important sink of carbon dioxide.

Trend analysis for the PAZ region (Supplementary Figure 3, Supplementary Table 1) produces comparable results. Annual trends are indistinguishable between the 3 SOCAT datasets as well as between the SOM-FFN product, both full and sampled. It could be that the greater extent of the PAZ northward yields better agreement between the datasets and the SOM-FFN product. All annual trends are also below the atmospheric trend. Summer and winter trends for the PAZ are consistent with results for the SPSS biome with winter trends being larger than summer trends, most significantly for the SOCAT-DP and SOM-FFN datasets. While actual trend values are different from those shown in Fig. 2, the results show that the relationship between trends for the 3 SOCAT datasets are indistinguishable for both seasons and annual analyses.

400

5. DPT as a pCO_2 evaluation point for biogeochemical profiling floats

Starting in late 2014, autonomous biogeochemical profiling floats have been deployed as part of the SOCCOM project, and as of December 2017, ten floats had traveled through or were approaching the Drake Passage region (Figure 7a). These floats offer a new opportunity to complement our oceanographic
405 understanding that has been developed primarily with traditional shipboard observations. Results above show that a lack of observations outside of the Drake Passage region may contribute to the large uncertainties in both seasonality and trends, which limits the conclusions we are able to make with currently available shipboard data. As floats provide autonomous, near real-time observations covering existing spatial and temporal gaps throughout the Southern Ocean and ship-based systems provide high
410 density observations at higher accuracy (±2.7% or 11 μatm at a pCO_2 of 400 μatm for floats compared to ±2 μatm for ships), there is great potential for these two platforms to work in concert to provide a whole Southern Ocean carbon observing system. However, there are limitations of float observations notably the indirect estimate of pCO_2 from pH and the requirement to adjust the sensor calibrations post-deployment by reference to deep (near 1500 m) pH values estimated from multiple linear regression equations fitted to
415 high quality, spectrophotometric pH observations made on repeat hydrography cruises [Williams et al., 2016; 2017; Johnson et al., 2016; 2017]. Further comparisons between float-estimated pCO_2 and shipboard observations is clearly warranted, and the complementary strengths of the Drake Passage Time-series make it an ideal dataset to help address these issues.

420 Here we utilize the underway Drake Passage Time-series pCO_2 data to conduct comparisons to nearby SOCCOM floats, considering both seasonality as well as fine-scale crossovers. Note that in this section of the analysis we utilize data only from the Drake Passage Time-series (available at nodc.noaa.gov/ocads/data) instead of the SOCATv5 dataset because SOCAT data are not available after 2016 at the time of writing.

425

A strong benefit of autonomous observation systems is their ability to sample regions and times that are not often surveyed by ships. SOCCOM floats collect data throughout the year, and especially important are the

additional observations in austral winter, a time when there are limited opportunities for ship-based measurements. While currently only two full years of data are available from floats within the Drake Passage (2016-2017) they span the full width of the region (Figure 7a) and are able to observe during each month of the year. A seasonal comparison of monthly mean pCO_2 values for the DPT data and float pCO_2 estimates within the defined Drake Passage region show that both platforms capture the expected seasonal cycle for the subpolar Southern Ocean with a wintertime peak and summertime low (Figure 7b). All datasets shown have been adjusted to 2017 using the mean atmospheric trend (1.95 μatm yr^{-1}) [Dlugokencky et al., 2015], and thus mean values are higher than shown in the seasonal curves of Fig. 2. Standard error shading on the seasonal cycles (Figure 7b) includes considerations of measurement accuracy as this differs substantially between these two platforms. Shading represents 1 standard error accounting for the spatial and temporal heterogeneity of the sample and measurement error (2.7% or ±11 μatm at a pCO_2 of 400 μatm for floats; ±2 μatm for DPT data), combined using the square root of the sum of squares.

The seasonal cycle derived from float-estimated pCO_2 has a larger seasonal amplitude compared to the DPT data from 2002-2017, due to an earlier and much lower observed summertime minimum. The difference in summertime minima is smaller however when DPT data from only 2016 and 2017 are considered (Figure 7b). The remaining difference between the floats and the DPT 2016-2017 data might be an artifact of the specific locations sampled, as floats and ships are not exactly synchronous, as well as the conditions specific to 2016 and 2017. In summer 2016 for example, the floats appear to have captured a strong phytoplankton bloom to the north and upstream of the Drake Passage, not captured by the DPT, that resulted in strong inorganic carbon uptake and low pCO_2; the floats did not sample in the southern region where pCO_2 is substantially higher in the early spring (Figure 8). However, there is no indication from the 2002-2017 seasonal cycle that this low excursion of the pCO_2 persists when looking at the entire Drake Passage region (Figure 7b). Since phytoplankton blooms typically progress southward during spring [Carranza and Gille, 2015] this difference in phasing likely results from the floats sampling preferentially the earlier northern uptake.

Underway Drake Passage Time-series pCO_2 data in the SPSS biome has a large range, often spanning over

100 µatm each month as shown in the time-series in Fig. 8, largely related to the 10°C temperature gradient and associated physical and biological dynamics that are captured over the region. pCO_2 from all floats east of 90°W and west of 55°W are also plotted on the time-series (Figure 8, diamonds) with the reported pCO_2 value being an average for all depths shallower than 20 m. Float-based pCO_2 surface estimates largely fall within the range of the direct underway pCO_2 observations, however notable differences do exist when spatial and temporal differences are taken into consideration. Float estimates from the central Drake Passage in winter (JJA) 2017 (Figure 8b) are higher than nearby DPT observations, though cruise data do not precisely overlap in time. Overall, the range of the DPT observations are far larger than the range of estimated pCO_2 from floats inside the Drake Passage region because they regularly span across the full width of the Drake Passage where meridional decorrelation length scales are relatively short [Eveleth et al., 2017]. Conversely, floats tend to sample along the path of the ACC.

As floats offer autonomous, frequent observations and ships offer data of the highest quality, it is ideal for these two platforms to work in partnership. Analysis of direct comparisons between DPT data and SOCCOM floats at crossover points indicates more precisely this potential (Figure 9). As of December 2017, there have been six occurrences of floats surfacing near DPT observations within a window of 75 km, 3 days, and have a reported SST within 0.3°C of each other (Figure 9a). This window is consistent with the crossover criteria used by the SOCAT community to quality control shipboard data [Pfeil et al., 2013; Olsen et al., 2013]. Figure 9a shows locations of the floats and the nearby DPT observations that fit this crossover window. As DPT offers high frequency observations, all available measurements over the 3-day window are shown (Figure 9b). Also indicated are DPT observations that crossover within a 50km and 2-day window and 25km and 1-day window (Figure 9b, black 'x' and squares respectively), both also with the 0.3°C SST criteria.

This comparison of the calculated pCO_2 from the floats and observed DPT pCO_2 reveals a broad correspondence (passing through the 1:1 line) in all 6 crossover instances within the ±2.7% relative standard uncertainty of the SOCCOM float measurements and ±2 µatm DPT uncertainty (Figure 9b shading). While all float crossovers do intersect the 1:1 line given their stated uncertainties, these

comparisons reveal the large range of pCO_2 captured by high-frequency shipboard measurements in a relatively small region and illustrates that this range cannot be fully captured by floats surfacing only once every 10 days. Further investigation of crossovers in the entire Southern Ocean region is needed; the DPT provides the most likely occurrence for this, although other regions with frequent ship traffic and autonomous platforms with biogeochemical capabilities should also be utilized when feasible. Additional post-deployment data quality checks using the underway surface pCO_2 data from DPT and other ship-based programs should be conducted, and more thorough assessments could be achieved if hydrocast observations were planned to occur in the vicinity of a passing biogeochemical float. Such coordinated efforts would significantly advance monitoring of the carbon cycle in the Southern Ocean.

6. Conclusions

The Drake Passage Time-series illustrates the large variability of surface ocean pCO_2 and exemplifies the value of sustained observations for understanding changing ocean carbon uptake in the Southern Ocean. This is the only location where carbon measurements throughout the entire annual cycle in the subpolar Southern Ocean have been made regularly over the past two decades. The available observations to date indicate that the Drake Passage seasonal cycle is representative of the seasonality observed for the entire SPSS biome, but increased observations outside of the Drake Passage, specifically during austral winter, are needed to provide a more robust comparison. Uncertainties in the seasonality for all datasets studied remain considerable given the dynamic nature of this region and the short time-series considered. Specifically, a lack of winter data in all years limits the direct conclusions for differences between the Drake Passage and the larger SPSS biome where we see a discrepancy in the timing of the winter maxima. These findings can direct specific goals for focus regions of future observations. Specifically, insufficient wintertime data in regions outside of the Drake Passage limits our assessment of how representative Drake Passage data is of the larger subpolar region.

The magnitude of interannual variability is comparable for SOCAT pCO_2 data within and outside of the Drake Passage region of the SPSS biome, a finding that conflicts with results from previous modeling and analysis of the SOM-FFN product. A clear idea of whether the Drake Passage is more or less variable in

pCO_2 will require increased data, particularly during the austral winter, outside of the Drake Passage. Given these data restrictions, the representativeness of the larger SPSS biome is also investigated using the SOM-FFN product. Within this gap-filled data product, monthly anomalies in the Drake Passage region are representative of broad swaths of the Southern Ocean, specifically regions upstream of the Drake Passage, but strong relationships are also evident in regions in the Indian Ocean sector of the Southern Ocean. Consistent with this finding, estimates of long-term trends do not change substantially if observations in the Drake Passage are removed from the SOM-FFN analysis. Across approaches to data analysis, trends in annual oceanic pCO_2 trends for 2002-2016 are less than the atmospheric pCO_2 trend, confirming previous findings that the Southern Ocean has, on average, been a growing sink for atmospheric carbon over this period.

Comparisons between underway DPT measurements and SOCCOM float estimates taken within the Drake Passage show broad agreement, while a fine-scale crossover investigation demonstrates their direct correspondence given uncertainty ranges for SOCCOM float pCO_2 estimates. Continuation of high-temporal measurements of the DPT in addition to expanded programs to target floats with both underway observations and frequent hydrocasts serving as independent datasets for post-deployment, will provide high-value comparisons, improving community confidence in float-based pCO_2 estimates. Coordinated monitoring efforts that combine a well-calibrated array of autonomous biogeochemical floats with a robust ship-based observational network will improve and expand monitoring of the carbon cycle in the Southern Ocean in the future.

Acknowledgements. We are grateful for funding from NSF (PLR-1543457, OCE-1558225, OCE-1155240), NOAA (NA12OAR4310058), and NASA (NNX17AK19G). NCAR is sponsored by the National Science Foundation. We acknowledge support from the Space Science and Engineering Center of University of Wisconsin – Madison and Columbia University. The authors are especially grateful for the efforts of the marine and science support teams of the ARSV Laurence M. Gould, particularly Timothy Newberger, Kevin Pedigo, Bruce Felix, and Andy Nunn. Underway DPT measurements presented in this manuscript are archived at NOAA's National Centers for Environmental Information (https://www.nodc.noaa.gov/ocads/oceans/VOS_Program/LM_gould.html). The Surface Ocean CO_2 Atlas (SOCAT) is an international effort, supported by the International Ocean Carbon Coordination Project (IOCCP), the Surface Ocean Lower Atmosphere Study (SOLAS), and the Integrated Marine Biogeochemistry and Ecosystem Research program (IMBER), to deliver a uniformly quality-controlled surface ocean CO_2 database. The many researchers and funding agencies responsible for the collection of data and quality control are thanked for their contributions to SOCAT. Float data were collected and made freely available by the Southern Ocean Carbon and Climate Observations and Modeling (SOCCOM)

Project funded by the National Science Foundation, Division of Polar Programs (NSF PLR-1425989), supplemented by NASA, and by the International Argo Program and the NOAA programs that contribute to it. (http://www.argo.ucsd.edu, http://argo.jcommops.org). The Argo Program is part of the Global Ocean Observing System.

References

Bakker, D. C. E., Pfeil, B. Landa, C. S., Metzl, N., O'Brien, K. M., Olsen, A., Smith, K., Cosca, C., Harasawa, S., Jones, S. D., Nakaoka, S., Nojiri, Y., Schuster, U., Steinhoff, T., Sweeney, C., Takahashi, T., Tilbrook, B., Wada, C., Wanninkhof, R., Alin, S. R., Balestrini, C. F., Barbero, L., Bates, N. R., Bianchi, A. A., Bonou, F., Boutin, J., Bozec, Y., Burger, E. F., Cai, W.-J., Castle, R. D., Chen, L., Chierici, M., Currie, K., Evans, W., Featherstone, C., Feely, R. A., Fransson, A., Goyet, C., Greenwood, N., Gregor, L., Hankin, S., Hardman-Mountford, N. J., Harlay, J., Hauck, J., Hoppema, M., Humphreys, M. P., Hunt, C. W., Huss, B., Ibánhez, J. S. P., Johannessen, T., Keeling, R., Kitidis, V., Körtzinger, A., Kozyr, A., Krasakopoulou, E., Kuwata, A., Landschützer, P., Lauvset, S. K., Lefèvre, N., Lo Monaco, C., Manke, A., Mathis, J. T., Merlivat, L., Millero, F. J., Monteiro, P. M. S., Munro, D. R., Murata, A., Newberger, T., Omar, A. M., Ono, T., Paterson, K., Pearce, D., Pierrot, D., Robbins, L. L., Saito, S., Salisbury, J., Schlitzer, R., Schneider, B., Schweitzer, R., Sieger, R., Skjelvan, I., Sullivan, K. F., Sutherland, S. C., Sutton, A. J., Tadokoro, K., Telszewski, M., Tuma, M., Van Heuven, S. M. A. C., Vandemark, D., Ward, B., Watson, A. J., Xu, S. (2016) A multi-decade record of high quality fCO2 data in version 3 of the Surface Ocean CO2 Atlas (SOCAT). Earth System Science Data 8: 383-413. doi:10.5194/essd-8-383-2016.

Carranza, M. M., and Gille S. T. (2015), Southern Ocean wind-driven entrainment enhances satellite chlorophyll-a through the summer, *J. Geophys. Res. Oceans, 120*, 304–323, doi:10.1002/2014JC010203.

Carter, B. R., Williams, N. L., Gray, A. R., & Feely, R. A. (2016). Locally interpolated alkalinity regression for global alkalinity estimation. *Limnology and Oceanography: Methods*, *14*(4), 268-277.

Ciais, P., and C. Sabine (2013), Chapter 6: Carbon and other biogeochemical cycles, in *Climate Change 2013: The Physical Science Basis. Contribution of Working Group I to the Fifth Assessment Report of the Intergovernmental Panel on Climate Change*, edited by T. F. Stocker et al., p. 1535, Cambridge Univ. Press, Cambridge, U. K., and New York.

Dlugokencky, E.J., K.A. Masarie, P.M. Lang, and P.P. Tans (2015), NOAA Greenhouse Gas Reference from Atmospheric Carbon Dioxide Dry Air Mole Fractions from the NOAA ESRL Carbon Cycle Cooperative Global Air Sampling Network. Data Path: ftp://aftp.cmdl.noaa.gov/data/trace_gases/co2/flask/surface/

Dlugokencky, E. and P. Tans, 2017. NOAA/ESRL, www.esrl.noaa.gov/gmd/ccgg/trends/ (accessed September 15, 2017).

Eveleth, R., Cassar, N., Doney, S. C., Munro, D. R., & Sweeney, C. (2017). Biological and physical controls on O2/Ar, Ar and pCO2 variability at the Western Antarctic Peninsula and in the Drake Passage. *Deep Sea Research Part II: Topical Studies in Oceanography*, *139*, 77-88.

Fay, A. R., and McKinley, G. A. (2013). Global trends in surface ocean pCO2 from in situ data. *Global Biogeochemical Cycles*, *27*(2), 541-557.

Fay, A. R., and G. A. McKinley (2014), Global open-ocean biomes: Mean and temporal variability, *Earth Syst. Sci. Data*, *6*(2), 273–284, doi:10.5194/essd-6-273-2014.

Fay, A. R., McKinley, G. A., & Lovenduski, N. S. (2014). Southern Ocean carbon trends: Sensitivity to methods. *Geophysical Research Letters*, *41*(19), 6833-6840.

Freeman, N.M, and N.S. Lovenduski, (2016) Mapping the Antarctic Polar Front: weekly realizations from 2002 to 2014, Earth System Science Data, 8, 191-198, doi:10.5194/essd-8-191-2016.

Freeman, N.M., N.S. Lovenduski, and P.R. Gent, (2016) Temporal variability in the Antarctic Polar Front (2001-2014), Journal of Geophysical Research: Oceans, 121, 7263-7276, doi:10.1002/2016JC012145.

Frölicher, T. L., Sarmiento, J. L., Paynter, D. J., Dunne, J. P., Krasting, J. P., & Winton, M. (2015). Dominance of the Southern Ocean in anthropogenic carbon and heat uptake in CMIP5 models. *Journal of Climate*, *28*(2), 862-886.

Gregor, L., S. Kok, & P. M. S. Monteiro, (2018) Interannual drivers of the seasonal cycle of CO_2 in the Southern Ocean. Biogeosciences, 15, 2361 2378.

Gruber, N., Gloor, M., Mikaloff Fletcher, S. E., Doney, S. C., Dutkiewicz, S., Follows, M. J., Gerber, M., Jacobson, A. R., Joos, F., Lindsay, K., Menemenlis, D., Mouchet, A., Müller, S. A., Sarmiento, J. L., and Takahashi, T, (2009) Oceanic sources, sinks, and transport of atmospheric CO_2, Global Biogeochem. Cy., 23, GB1005, doi:10.1029/2008GB003349.

Hoppema, M., Velo, A., Heuven, S. V., Tanhua, T., Key, R. M., Lin, X., Sabine, C. L. (2009). Consistency of cruise data of the CARINA database in the Atlantic sector of the Southern Ocean. *Earth System Science Data*, *1*(1), 63-75.

Johnson, K.S., Jannasch, H.W., Coletti, L.J., Elrod, V.A., Martz, T.R., Takeshita, Y., Carlson, R.J. and Connery, J.G. (2016) Deep-Sea DuraFET: A pressure tolerant pH sensor designed for global sensor networks. *Analytical Chemistry*, *88*(6), pp.3249-3256.

Johnson, K. S., Plant, J. N., Coletti, L. J., Jannasch, H. W., Sakamoto, C. M., Riser, S. C., Talley, L. D. (2017) Biogeochemical sensor performance in the SOCCOM profiling float array. *Journal of Geophysical Research: Oceans doi:10.1002/2017JC012838*.

Landschützer, P., N. Gruber, D. C. E. Bakker, and U. Schuster (2014a), Recent variability of the global ocean carbon sink, *Global Biogeochem. Cycles*, *28*, 927–949, doi:10.1002/2014GB004853.

Landschützer, P., Gruber, N., Bakker, D. C. E., Schuster, U. (2014b) An observation-based global monthly gridded sea surface pCO2 product from 1998 through 2011 and its monthly climatology, available on: http://cdiac.ornl.gov/oceans/SPCO2_1998_2011_ETH_SOM_FFN.html.

Landschützer, P., Gruber, N., Haumann, F., Rödenbeck, C., Bakker, D., van Heuven, S., Hoppema, M., Metzl, N., Sweeney, C., Takahashi, T., Tilbrook, B., and Wanninkhof, R. (2015a) The reinvigoration of the Southern Ocean carbon sink, Science, 349, 1221–1224.

Landschützer, P., N. Gruber, & D.C.E. Bakker. (2015b). A 30 years observation-based global monthly gridded sea surface pCO2 product from 1982 through 2011. http://cdiac.ornl.gov/ftp/oceans/SPCO2_1982_2011_ETH_SOM_FFN. Carbon Dioxide Information Analysis Center, Oak Ridge National Laboratory, US Department of Energy, Oak Ridge, Tennessee. doi: 10.3334/CDIAC/OTG.SPCO2_1982_2011_ETH_SOMFFN

Landschützer, P., Gruber, N., Bakker, D. C. E. (2016) Decadal variations and trends of the global ocean carbon sink, Global Biogeochemical Cycles, 30, doi:10.1002/2015GB005359

Landschützer, P., Gruber, N., Bakker, D. C. E. (2017). An updated observation-based global monthly gridded sea surface pCO2 and air-sea CO2 flux product from 1982 through 2015 and its monthly climatology (NCEI Accession 0160558). Version 2.2. NOAA National Centers for Environmental

Information. Dataset. [2017-07-11]: available at https://www.nodc.noaa.gov/ocads/oceans/SPCO2_1982_2015_ETH_SOM_FFN.html

Le Quéré, C., Rödenbeck, C., Buitenhuis, E. T., Conway, T. J., Langenfelds, R., Gomez, A., Labuschagne, C., Ramonet, M., Nakazawa, T., Metzl, N., Gillett, N., and Heimann, M. (2007) Satuation of the Southern Ocean CO_2 sink due to recent climate change, Science, 316, 1735–1738, doi:10.1126/science.1136188.

Le Quéré, C., R. M. Andrew, J. G. Canadell, S. Sitch, J. I. Korsbakken, G. P. Peters, A. C. Manning, T. A. Boden, P. P. Tans, R. A. Houghton, R. F. Keeling, S. Alin, O. D. Andrews, P. Anthoni, L. Barbero, L. Bopp, F. Chevallier, L. P. Chini, P. Ciais, K. Currie, C. Delire, S. C. Doney, P. Friedlingstein, T. Gkritzalis, I. Harris, J. Hauck, V. Haverd, M. Hoppema, K. K. Goldewijk, A. K. Jain, E. Kato, A. Körtzinger, P. Landschützer, N. Lefèvre, A. Lenton, S. Lienert, D. Lombardozzi, J. R. Melton, N. Metzl, F. Millero, P. M. S. Monteiro, D. R. Munro, J. E. M. S. Nabel, S. Nakaoka, K. O'Brien, A. Olsen, A. M. Omar, T. Ono, D. Pierrot, B. Poulter, C. Rödenbeck, J. Salisbury, U. Schuster, J. Schwinger, R. Séférian, I. Skjelvan, B. D. Stocker, A. J. Sutton, T. Takahashi, H. Tian, B. Tilbrook, I. T. van der Laan-Luijkx, G. R. van der Werf, N. Viovy, A. P. Walker, A. J. Wiltshire, S. Zaehle (2016), Earth System Science Data, DOI:10.5194/essd-8-605-2016.

Le Quéré, C., Andrew, R. M., Friedlingstein, P., Sitch, S., Pongratz, J., Manning, A. C., Korsbakken, J. I., Peters, G. P., Canadell, J. G., Jackson, R. B., Boden, T. A., Tans, P. P., Andrews, O. D., Arora, V. K., Bakker, D. C. E., Barbero, L., Becker, M., Betts, R. A., Bopp, L., Chevallier, F., Chini, L. P., Ciais, P., Cosca, C. E., Cross, J., Currie, K., Gasser, T., Harris, I., Hauck, J., Haverd, V., Houghton, R. A., Hunt, C. W., Hurtt, G., Ilyina, T., Jain, A. K., Kato, E., Kautz, M., Keeling, R. F., Klein Goldewijk, K., Körtzinger, A., Landschützer, P., Lefèvre, N., Lenton, A., Lienert, S., Lima, I., Lombardozzi, D., Metzl, N., Millero, F., Monteiro, P. M. S., Munro, D. R., Nabel, J. E. M. S., Nakaoka, S.-I., Nojiri, Y., Padín, X. A., Peregon, A., Pfeil, B., Pierrot, D., Poulter, B., Rehder, G., Reimer, J., Rödenbeck, C., Schwinger, J., Séférian, R., Skjelvan, I., Stocker, B. D., Tian, H., Tilbrook, B., van der Laan-Luijkx, I. T., van der Werf, G. R., van Heuven, S., Viovy, N., Vuichard, N., Walker, A. P., Watson, A. J., Wiltshire, A. J., Zaehle, S., and Zhu, D. (2017) Global Carbon Budget 2017, Earth Syst. Sci. Data Discuss., https://doi.org/10.5194/essd-2017-123, in review.

Lo Monaco, C., Metzl, N., Poisson, A., Brunet, C., & Schauer, B. (2005). Anthropogenic CO2 in the Southern Ocean: Distribution and inventory at the Indian-Atlantic boundary (World Ocean Circulation Experiment line I6). *Journal of Geophysical Research: Oceans*, *110*(C6).

Lo Monaco, C. L., Alvarez, M., Key, R. M., Lin, X., Tanhua, T., Tilbrook, B., Ríos, A. F. (2010). Assessing the internal consistency of the CARINA database in the Indian sector of the Southern Ocean. *Earth System Science Data*, *2*(1), 51.

Lovenduski, N. S., Gruber, N., & Doney, S. C. (2008). Toward a mechanistic understanding of the decadal trends in the Southern Ocean carbon sink. *Global Biogeochemical Cycles*, *22*(3).

Lovenduski, N. S., A. R. Fay, and G. A. McKinley (2015), Observing multidecadal trends in Southern Ocean CO2 uptake: What can we learn from an ocean model?, *Global Biogeochem. Cycles*, *29*(4), 416–426, doi:10.1002/2014GB004933.

Majkut, J. D., Carter, B. R., Frölicher, T. L., Dufour, C. O., Rodgers, K. B., & Sarmiento, J. L. (2014). An observing system simulation for Southern Ocean carbon dioxide uptake. *Phil. Trans. R. Soc. A*, *372*(2019), 20130046.

McKinley, G. A., Fay, A. R., Lovenduski, N. S., & Pilcher, D. J. (2017). Natural variability and anthropogenic trends in the ocean carbon sink. *Annual review of marine science*, *9*, 125-150.

Metzl, N., Tilbrook, B., & Poisson, A. (1999). The annual fCO_2 cycle and the air'sea CO_2 flux in the sub-Antarctic Ocean. *Tellus B: Chemical and Physical Meteorology*, *51*(4), 849-861.

Metzl, N. (2009). Decadal increase of oceanic carbon dioxide in Southern Indian Ocean surface waters (1991–2007). *Deep Sea Research Part II: Topical Studies in Oceanography*, *56*(8), 607-619.

Munro, D. R., N. S. Lovenduski, T. Takahashi, B. B. Stephens, T. Newberger, and C. Sweeney (2015a), Recent evidence for a strengthening CO_2 sink in the Southern Ocean from carbonate system measurements in the Drake Passage (2002-2015), Geophys. Res. Lett., 42, 7623–7630, doi:10.1002/2015GL065194.

Munro, D. R., N. S. Lovenduski, B. B. Stephens, T. Newberger, K. R. Arrigo, T. Takahashi, P.D. Quay, J. Sprintall, N.M. Freeman, C. Sweeney (2015b), Estimates of net community production in the Southern Ocean determined from time-series observations (2002–2011) of nutrients, dissolved inorganic carbon, and surface ocean pCO_2 in Drake Passage, Deep Sea Res., Part II, 114, 49–63, doi:10.1016/j.dsr2.2014.12.014.

Olsen, A., N. Metzl, D. Bakker, K. O'Brien (2013), SOCAT QC cookbook for SOCAT participants; available at: https://www.socat.info/wp-content/uploads/2017/04/2015_SOCAT_QC_Cookbook_v3.pdf, last access: 01 November 2017.

Pfeil, B., Olsen, A., Bakker, D. C. E., Hankin, S., Koyuk, H., Kozyr, A., Malczyk, J., Manke, A., Metzl, N., Sabine, C. L., Akl, J., Alin, S. R., Bates, N., Bellerby, R. G. J., Borges, A., Boutin, J., Brown, P. J., Cai, W.-J., Chavez, F. P., Chen, A., Cosca, C., Fassbender, A. J., Feely, R. A., González-Dávila, M., Goyet, C., Hales, B., Hardman-Mountford, N., Heinze, C., Hood, M., Hoppema, M., Hunt, C. W., Hydes, D., Ishii, M., Johannessen, T., Jones, S. D., Key, R. M., Körtzinger, A., Landschützer, P., Lauvset, S. K., Lefèvre, N., Lenton, A., Lourantou, A., Merlivat, L., Midorikawa, T., Mintrop, L., Miyazaki, C., Murata, A., Nakadate, A., Nakano, Y., Nakaoka, S., Nojiri, Y., Omar, A. M., Padin, X. A., Park, G.-H., Paterson, K., Perez, F. F., Pierrot, D., Poisson, A., Rios, A. F., Santana-Casiano, J. M., Salisbury, J., Sarma, V. V. S. S., Schlitzer, R., Schneider, B., Schuster, U., Sieger, R., Skjelvan, I., Steinhoff, T., Suzuki, T., Takahashi, T., Tedesco, K., Telszewski, M., Thomas, H., Tilbrook, B., Tjiputra, J., Vandemark, D., Veness, T., Wanninkhof, R., Watson, A. J., Weiss, R., Wong, C. S., Yoshikawa-Inoue, H. (2013) A uniform, quality controlled Surface Ocean CO_2 Atlas (SOCAT), Earth System Science Data 5: 125-143.doi:10.5194/essd-5-125-2013.

Rödenbeck, C., Bakker, D. C., Gruber, N., Iida, Y., Jacobson, A. R., Jones, S., Park, G. H. (2015). Data-based estimates of the ocean carbon sink variability–first results of the Surface Ocean pCO_2 Mapping intercomparison (SOCOM). *Biogeosciences*, *12*, 7251-7278.

Sabine, C.L., Hankin, S., Koyuk, H., Bakker, D. C. E., Pfeil, B., Olsen, A., Metzl, N., Kozyr, A., Fassbender, A., Manke, A., Malczyk, J., Akl, J., Alin, S. R., Bellerby, R. G. J., Borges, A., Boutin, J., Brown, P. J., Cai, W.-J., Chavez, F. P., Chen, A., Cosca, C., Feely, R. A., González-Dávila, M., Goyet, C., Hardman-Mountford, N., Heinze, C., Hoppema, M., Hunt, C. W., Hydes, D., Ishii, M., Johannessen, T., Key, R. M., Körtzinger, A., Landschützer, P., Lauvset, S. K., Lefèvre, N., Lenton, A., Lourantou, A., Merlivat, L., Midorikawa, T., Mintrop, L., Miyazaki, C., Murata, A., Nakadate, A., Nakano, Y., Nakaoka, S., Nojiri, Y., Omar, A. M., Padin, X. A., Park, G.-H., Paterson, K., Perez, F. F., Pierrot, D., Poisson, A., Ríos, A. F., Salisbury, J., Santana-Casiano, J. M., Sarma, V. V. S. S., Schlitzer, R., Schneider, B., Schuster, U., Sieger, R., Skjelvan, I., Steinhoff, T., Suzuki, T., Takahashi, T., Tedesco, K., Telszewski, M., Thomas, H., Tilbrook, B., Vandemark, D., Veness, T., Watson, A. J., Weiss, R., Wong, C. S., Yoshikawa-Inoue, H. (2013) Surface Ocean CO2 Atlas (SOCAT) gridded data products. Earth System Science Data 5: 145-153. doi:10.5194/essd-5-145-2013.

Shadwick, E. H., Trull, T. W., Tilbrook, B., Sutton, A. J., Schulz, E., & Sabine, C. L. (2015). Seasonality of biological and physical controls on surface ocean CO_2 from hourly observations at the Southern Ocean Time Series site south of Australia. *Global Biogeochemical Cycles*, *29*(2), 223-238.

Sprintall, J., Chereskin, T. K., & Sweeney, C. (2012). High-resolution underway upper ocean and surface atmospheric observations in Drake Passage: Synergistic measurements for climate science. *Oceanography*, *25*(3), 70-81.

Takahashi, T., Sutherland, S. C., Sweeney, C., Poisson, A., Metzl, N., Tilbrook, B., Bates, N., Wanninkhof, R., Feely, R. F., Sabine, C., Olafsson, J., and Nojiri, Y. (2002) Global sea-air CO_2 flux based on climatological surface ocean pCO_2 and seasonal biological and temperature effects, Deep-Sea Res. Pt. II, 49, 1601–1622.

Takahashi, T., Sutherland, S., Wanninkhof, R., Sweeney, C., Feely, R., Chipman, D., Hales, B., Friederich, G., Chavez, F., Sabine, C., Watson, A., Bakker, D., Schuster, U., Metzl, N., Yoshikawa-Inoue, H., Ishii, M., Midorikawa, T., Nojiri, Y., Körtzinger, A., Steinhoff, T., Hoppema, M., Olafson, J., Arnarson, T., Tilbrook, B., Johannessen, T., Olsen, A., Bellerby, R., Wong, C., Delille, B., Bates, N., and de Baar, H. (2009) Climatological mean and decadal change in surface ocean pCO_2, and net sea-air CO_2 flux over the global oceans, Deep-Sea Res. Pt. II, 56, 554–577.

Takahashi, T., Sweeney, C., Hales, B., Chipman, D. W., Newberger, T., Goddard, J. G., Iannuzzi, R.A., & Sutherland, S. C. (2012). The changing carbon cycle in the Southern Ocean. *Oceanography*, *25*(3), 26-37.

Takahashi, T., Sutherland, S.C., Chipman, D. W., Goddard , J.G., Ho, C., Newberger, T., Sweeney, C., Munro, D.R. (2014). Climatoogical Distributions of pH, pCO2, Total CO2, Alkalinity, and CaCO3 Saturation in the Global Surface Ocean, and Temporal Changes at Selected Locations. *Marine Chemistry*, doi: 10.1016/j.jmarchem.2014.06.004..

van Heuven, S. M., Hoppema, M., Huhn, O., Slagter, H. A., & de Baar, H. J. (2011). Direct observation of increasing CO_2 in the Weddell Gyre along the Prime Meridian during 1973–2008. *Deep Sea Research Part II: Topical Studies in Oceanography*, *58*(25), 2613-2635.

Williams, N. L., Juranek, L. W., Johnson, K. S., Feely, R. A., Riser, S. C., Talley, L. D., Russell, J.L., Sarmiento, J.L. , & Wanninkhof, R. (2016). Empirical algorithms to estimate water column pH in the Southern Ocean. *Geophysical Research Letters*, *43*(7), 3415-3422.

Williams, N. L., Juranek, L. W., Feely, R. A., Johnson, K. S., Sarmiento, J. L., Talley, L. D., Riser, S. C. (2017). Calculating surface ocean pCO_2 from biogeochemical Argo floats equipped with pH: an uncertainty analysis. *Global Biogeochemical Cycles*, *31*(3), 591-604.

Xue, L., Gao, L., Cai, W. J., Yu, W., & Wei, M. (2015). Response of sea surface fugacity of CO_2 to the SAM shift south of Tasmania: Regional differences. *Geophysical Research Letters*, *42*(10), 3973-3979.

Figure Captions

Figure 1

Map of Subpolar seasonally stratified (SPSS) biome [Fay and McKinley 2014], defined at 1° x 1° resolution. The red line represents the mean location of the Antarctic Polar Front [Freeman and Lovenduski, 2016], interpolated to a 1° x 1° grid. The black box represents the Drake Passage region considered in this analysis.

Figure 2

Mean surface ocean pCO_2 seasonal cycle estimate for years 2002-2016, for the SPSS biome from each dataset, shown on an 18-month cycle, calculated from a time-series corrected to year 2002 (atmospheric trend of 1.95 μatm yr^{-1} removed). Shading represents 1 standard error for biome-scale monthly means driven by interannual variability; there is no error represented for SOM-FFN. Bar plot indicates the number of years containing observations in a given month (maximum of 15 years) for the SOCAT-DP SOCAT-noDP, and SOCAT-all datasets.

Figure 3

Data density of pCO_2 observations from the SOCATv5 dataset within each 1° x 1° gridcell. Data is restricted to years 2002-2016. Salinity values outside of 33.5-34.5 psu and observations within 50 km of land are omitted. (a) data from all months of the year; (b) data from only June, July, and August (austral winter). Gray lines designate boundary of SPSS biome and Drake Passage region for reference.

Figure 4

(a) Temporal evolution of deseasonalized, detrended monthly SOCAT-DP pCO_2 anomalies (gray bars) over 2002-2016, with 12-month running averages (black line) overlain. (b) Correlation between monthly SOCAT-DP pCO_2 anomalies and the pCO_2 anomalies estimated from the SOM-FFN-noDP product (created without the inclusion of Drake Passage data), for years 2002-2016 at each 1° x 1° grid cell. Gray shading represents areas where the correlation does not pass significance t-tests at $p<0.05$.

Figure 5

Surface ocean pCO_2 trends in the SPSS biome for years 2002-2016 (μatm yr^{-1}): SOCATv5 data within the Drake Passage box (gray); SOCATv5 data excluding data from the Drake Passage box (green); SOCATv5 (blue); SOM-FFN product (magenta); SOM-FFN pCO_2 product sampled as SOCATv5 data in the Drake Passage box (light pink). Figure includes annual trends (left), austral summer trends (center) and austral winter trends (right). SOCAT-noDP winter trend omitted because it did not contain a JJA value for every year of the time-series. For reference, the atmospheric pCO_2 trend during the 2002-2015 period (1.95 μatm yr^{-1}) is shown as a horizontal black line.

Figure 6

(a) Sea-air CO_2 flux and (b) pCO_2 averaged over the Southern Ocean SPSS biome, from the SOM-FFN pCO_2 product (blue) and that of the SOM-FFN-noDP product created without the inclusion of Drake Passage data (red). Trends and uncertainty values in corresponding colors.

Figure 7

(a) Trajectories of Drake Passage-transiting SOCCOM floats included in this analysis. Colored diamonds represent the location of surface measurements for each float. Data from floats collected east of 55°W and west of 90°W are not included in this analysis. Gray dots represent observations from the DPT. (b) Mean surface ocean pCO_2 seasonal cycle estimate for: black: underway Drake Passage Time-series data for years 2002-2016, purple: DPT for years 2016-2017 to match years covered by the floats, and orange: SOCCOM floats. Seasonal cycles are shown on an 18-month cycle, calculated from a monthly mean time-series with the atmospheric correction to year 2017. Shading represents 1 standard error accounting for the spatial and temporal heterogeneity of the sample and the measurement error (2.7% or ±11 μatm at a pCO_2 of 400 μatm for floats; ±2 μatm for DPT data) combined using the square root of the sum of squares.

Figure 8

(a) 2002-2017 underway DPT pCO_2 observations (circles) and surface pCO_2 estimates from SOCCOM floats overlain (diamonds; μatm), plotted versus latitude. (b) Same as (a) but plotted as January 2016 to December 2017.

Figure 9

(a) Map of SOCCOM floats with DPT crossovers within 75km, 3 days, and 0.3°C SST from coincident surface observations. (b) Calculated pCO_2 from SOCCOM float (x-axis) versus DPT underway pCO_2 observations (y-axis) for crossover float locations, with 1:1 line. Colors correspond to float number in Figure 7. Horizontal width of shading represents SOCCOM relative standard uncertainty, which is estimated at ±2.7% μatm; vertical shading is ±2 μatm uncertainty around DPT observations. Black 'x' and squares indicated crossovers within a smaller window (50km/2day/0.3°C SST and 25km/1day/0.3°C SST respectively).

Supplementary Table 1

Seasonal and annual trends as reported in Figure 5 and Supplementary Figure 3.

Supplementary Figure 1

Map of Polar-front Antarctic Zone (PAZ) which is defined at 1° x 1° resolution as the region between the Subantarctic front and the northern extent of sea ice [Williams et al., 2017]. The red line represents the boundaries of the location of the Subpolar seasonally stratified (SPSS) biome [Fay & McKinley, 2014]. The black box represents the Drake Passage region considered in the supplementary figures that follow.

Supplementary Figure 2

Mean surface ocean pCO_2 seasonal cycle estimate for years 2002-2016, for the PAZ region from each dataset, shown on an 18-month cycle, calculated from a time-series with the atmospheric trend removed (1.95 μatm yr^{-1}). Shading represents 1 standard error for biome-scale monthly means. Bar plot indicates the number of years containing observations in a given month (maximum of 15 years) for the SOCAT-DP SOCAT-noDP, and SOCAT-all datasets.

Supplementary Figure 3

Surface ocean pCO_2 trends in the PAZ region for years 2002-2016 ($\mu atm\ yr^{-1}$): SOCATv5 data within the Drake Passage box (gray); SOCATv5 data excluding data from the Drake Passage box (green); SOCATv5 (blue); SOM-FFN product (magenta); SOM-FFN pCO_2 product sampled as SOCATv5 data in the Drake Passage box (light pink). Figure includes annual trends (left), summer trends (center) and winter trends (right). SOCAT-noDP winter trend omitted because it did not contain a JJA value for every year of the time-series. For reference, the atmospheric pCO_2 trend during the 2002-2015 period (1.95 $\mu atm\ yr^{-1}$) is shown as a horizontal black line.

Figure 1

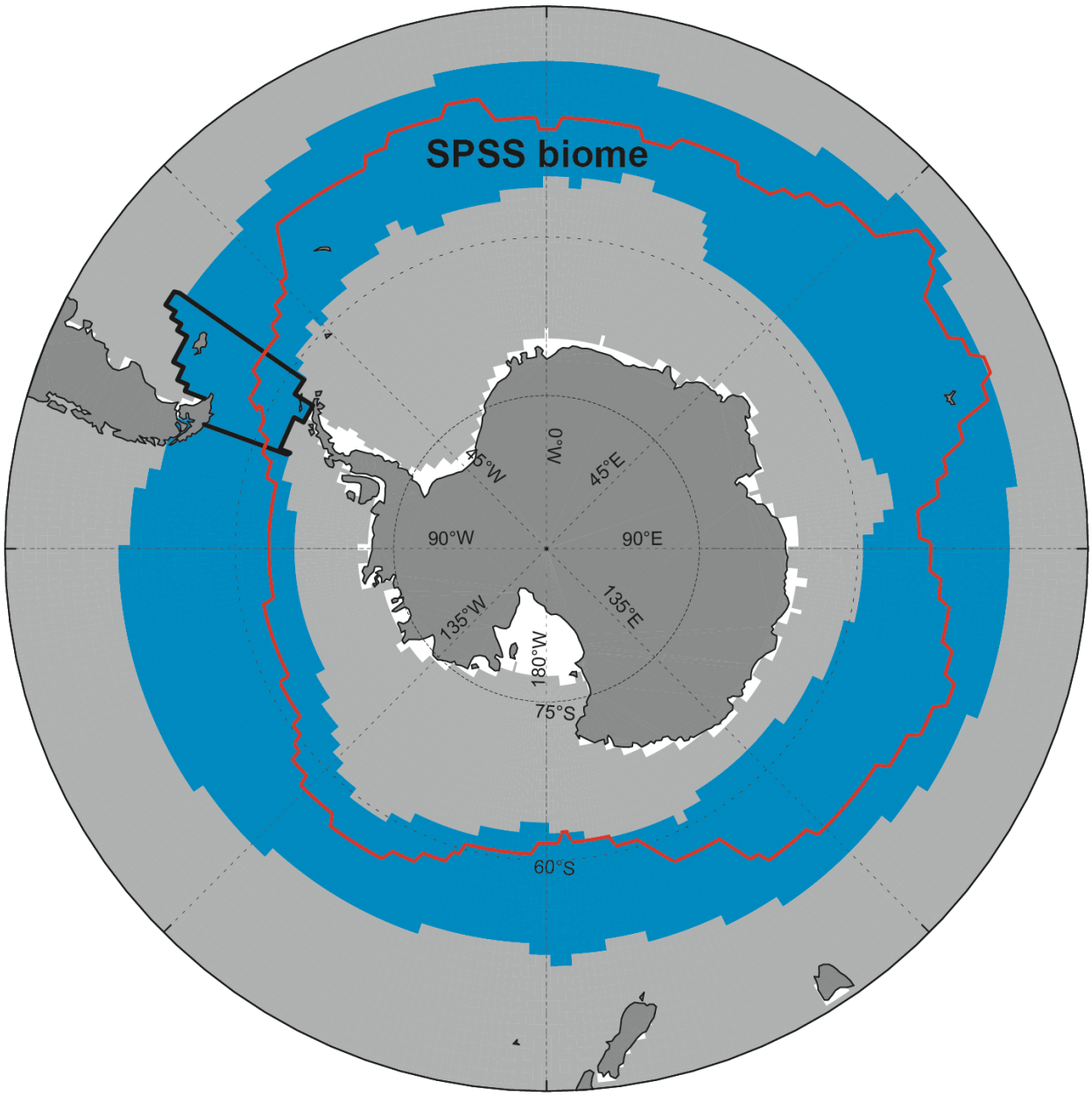

Figure 2

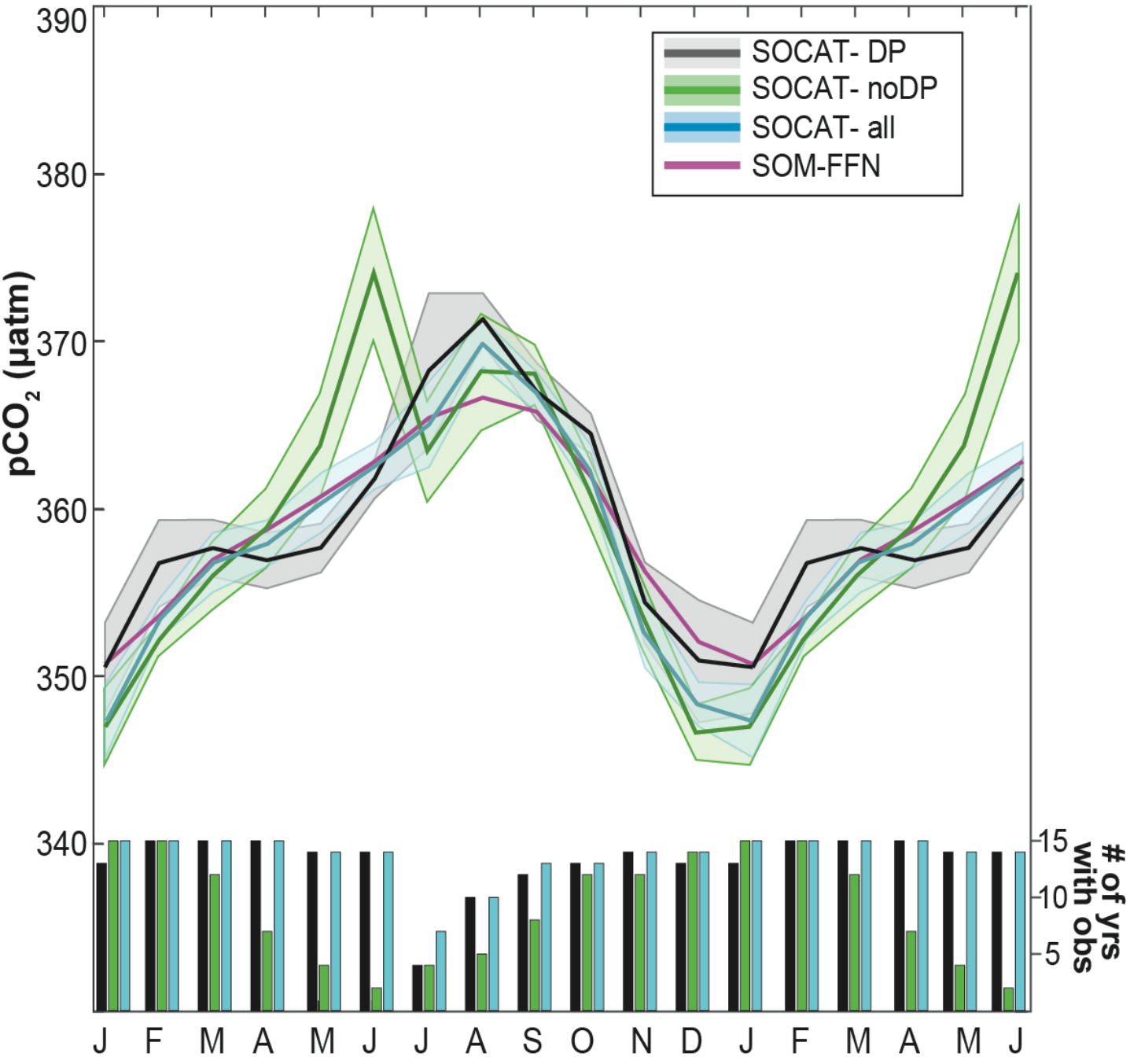
SOCAT- DP
SOCAT- noDP
SOCAT- all
SOM-FFN
pCO2 (µatm)
390
380
370
360
350
340
15
10
5
# of yrs with obs
J F M A M J J A S O N D J F M A M J

Figure 3

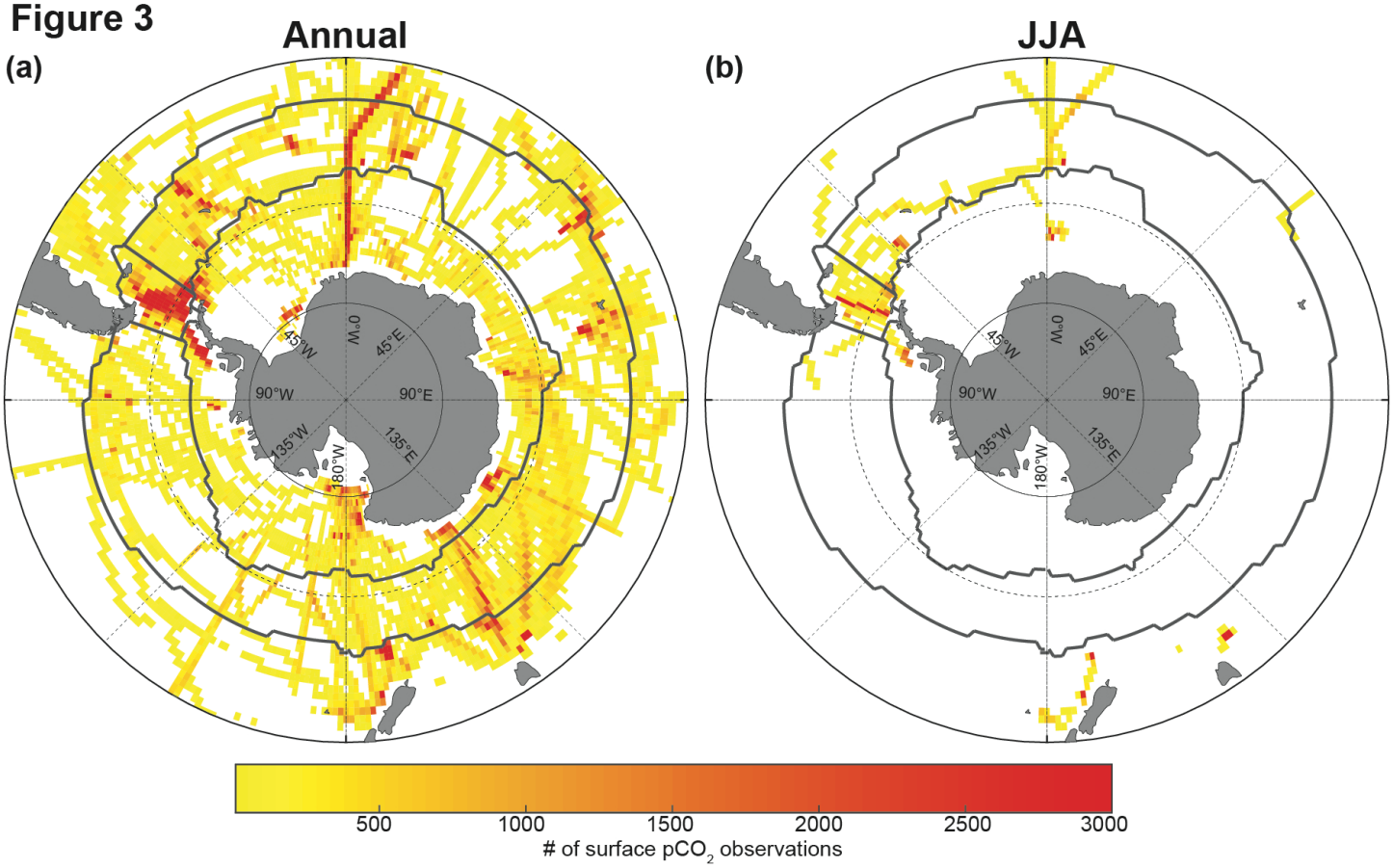
(a)
Annual
(b)
JJA
0°N
45°E
90°E
135°E
180°W
135°W
90°W
45°W
500
1000
1500
2000
2500
3000
# of surface pCO2 observations

Figure 4

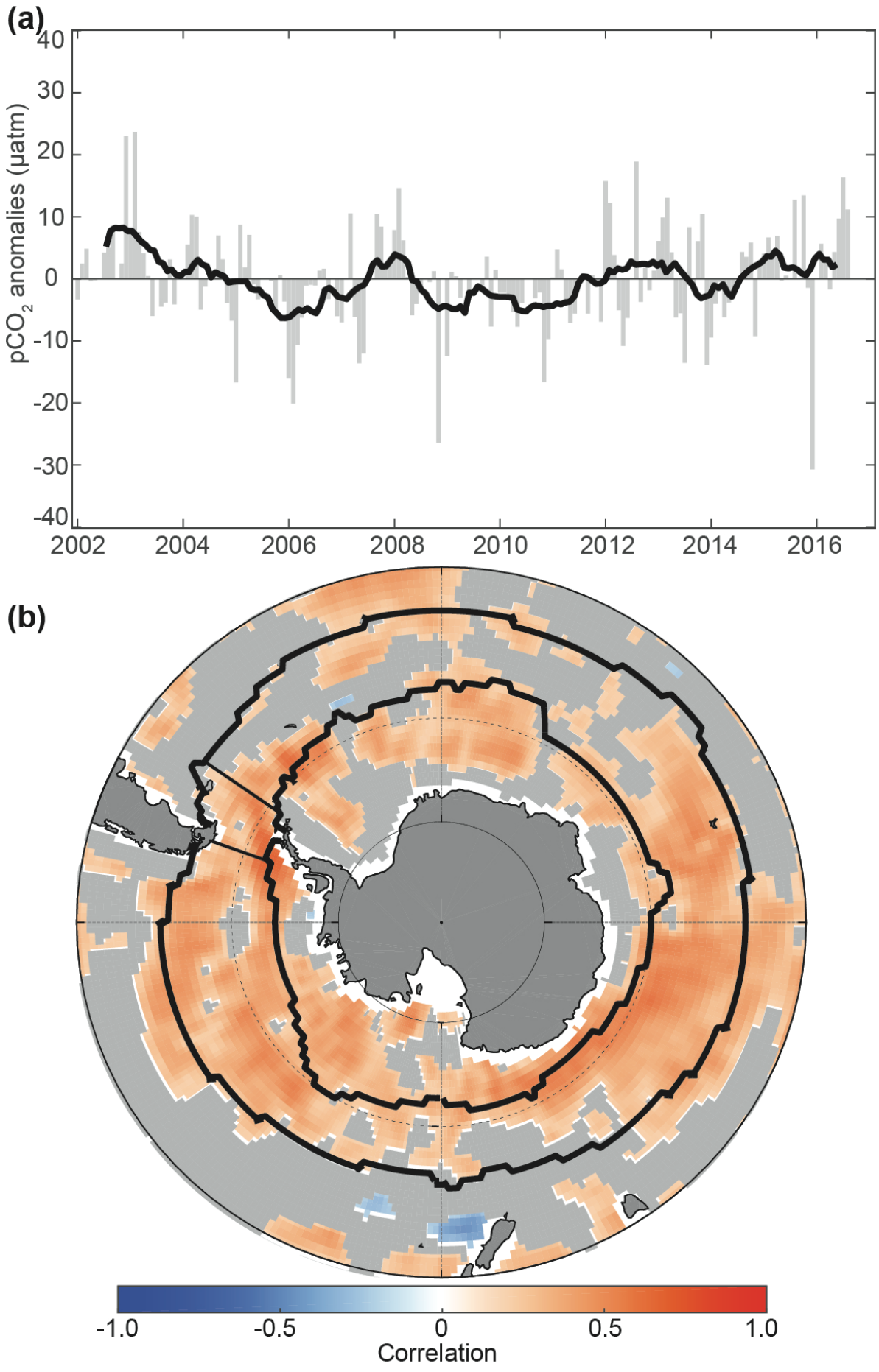
(a)
40
30
20
10
0
-10
-20
-30
-40
pCO2 anomalies (µatm)
2002
2004
2006
2008
2010
2012
2014
2016
(b)
-1.0
-0.5
0
0.5
1.0
Correlation

Figure 5

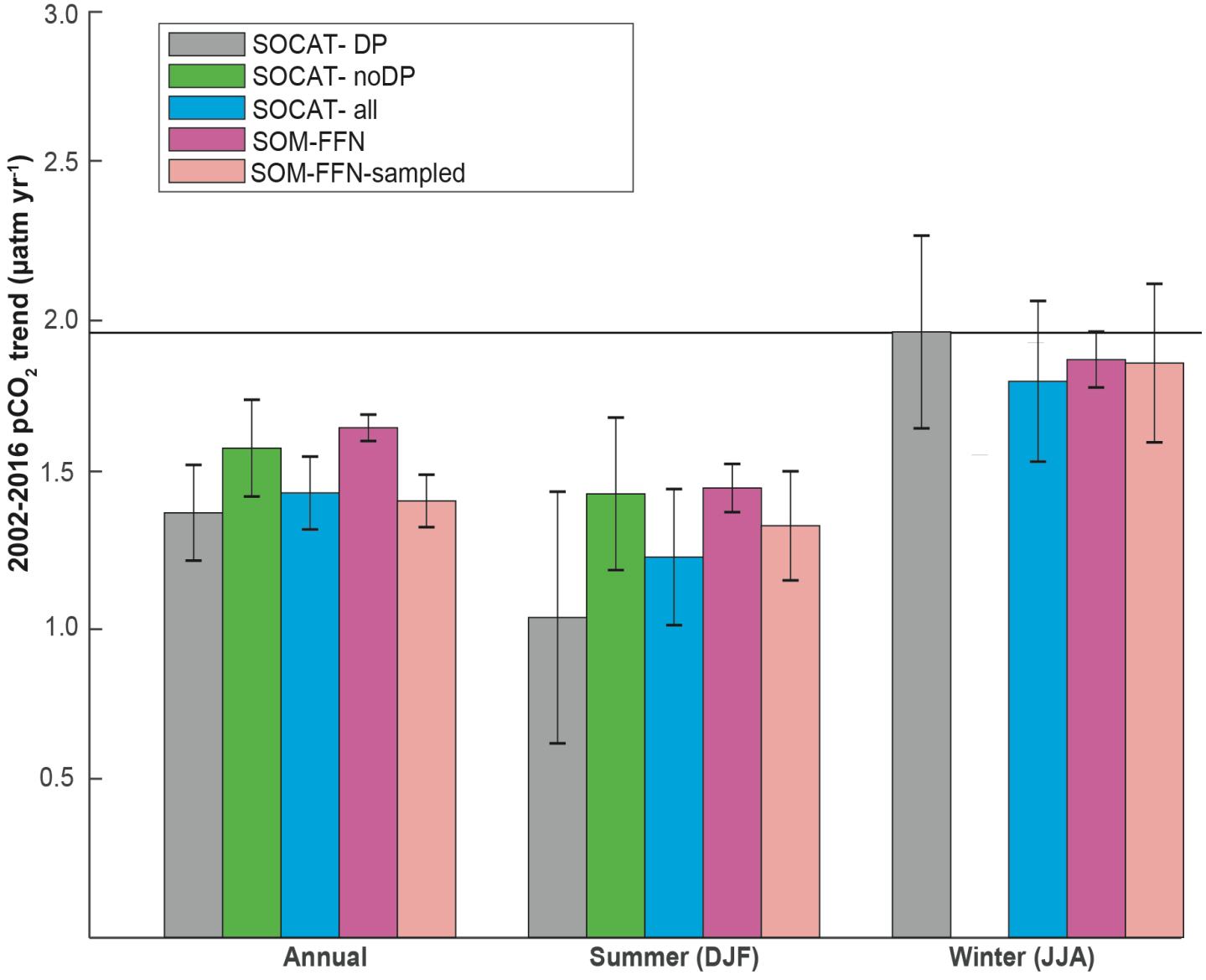
SOCAT- DP
SOCAT- noDP
SOCAT- all
SOM-FFN
SOM-FFN-sampled
2002-2016 pCO2 trend (µatm yr-1)
3.0
2.5
2.0
1.5
1.0
0.5
Annual
Summer (DJF)
Winter (JJA)

Figure 6

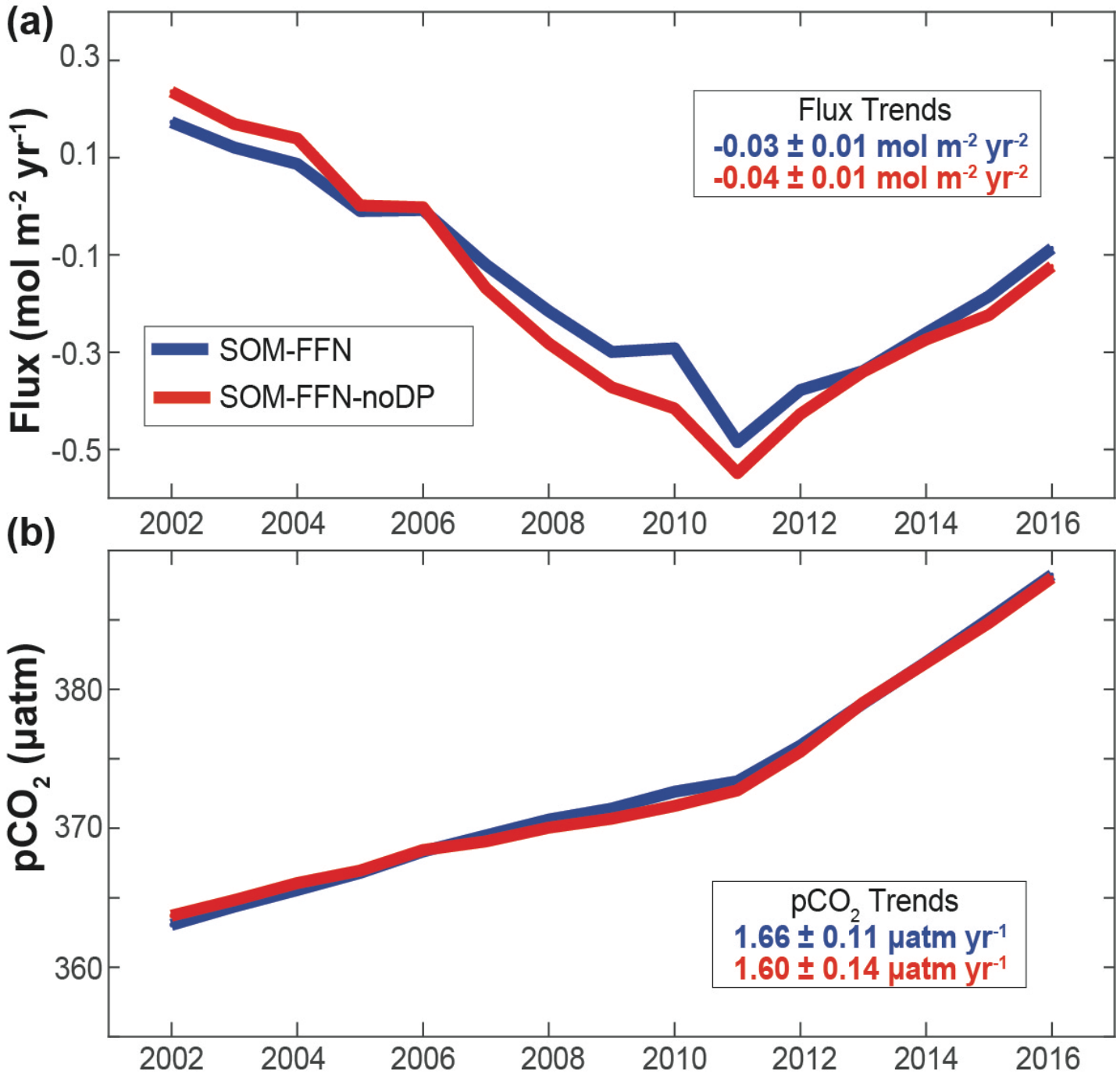
(a)
0.3
0.1
-0.1
-0.3
-0.5
Flux (mol m-2 yr-1)
Flux Trends
-0.03 ± 0.01 mol m-2 yr-2
-0.04 ± 0.01 mol m-2 yr-2
SOM-FFN
SOM-FFN-noDP
2002
2004
2006
2008
2010
2012
2014
2016
(b)
380
370
360
pCO2 (µatm)
pCO2 Trends
1.66 ± 0.11 µatm yr-1
1.60 ± 0.14 µatm yr-1
2002
2004
2006
2008
2010
2012
2014
2016

Figure 7

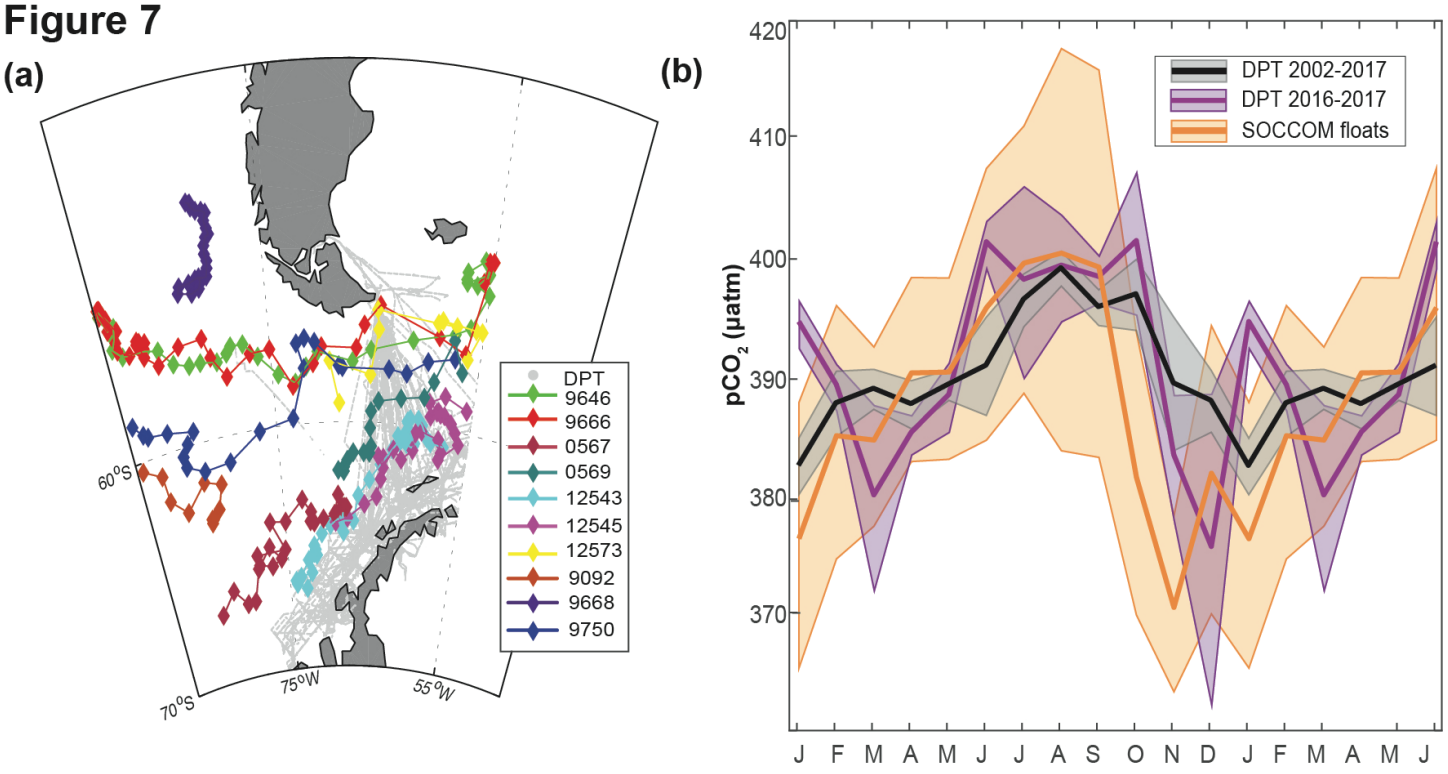
(a)
(b)
DPT
9646
9666
0567
0569
12543
12545
12573
9092
9668
9750
60°S
70°S
75°W
55°W
DPT 2002-2017
DPT 2016-2017
SOCCOM floats
pCO2 (µatm)
420
410
400
390
380
370
J F M A M J J A S O N D J F M A M J

Figure 8

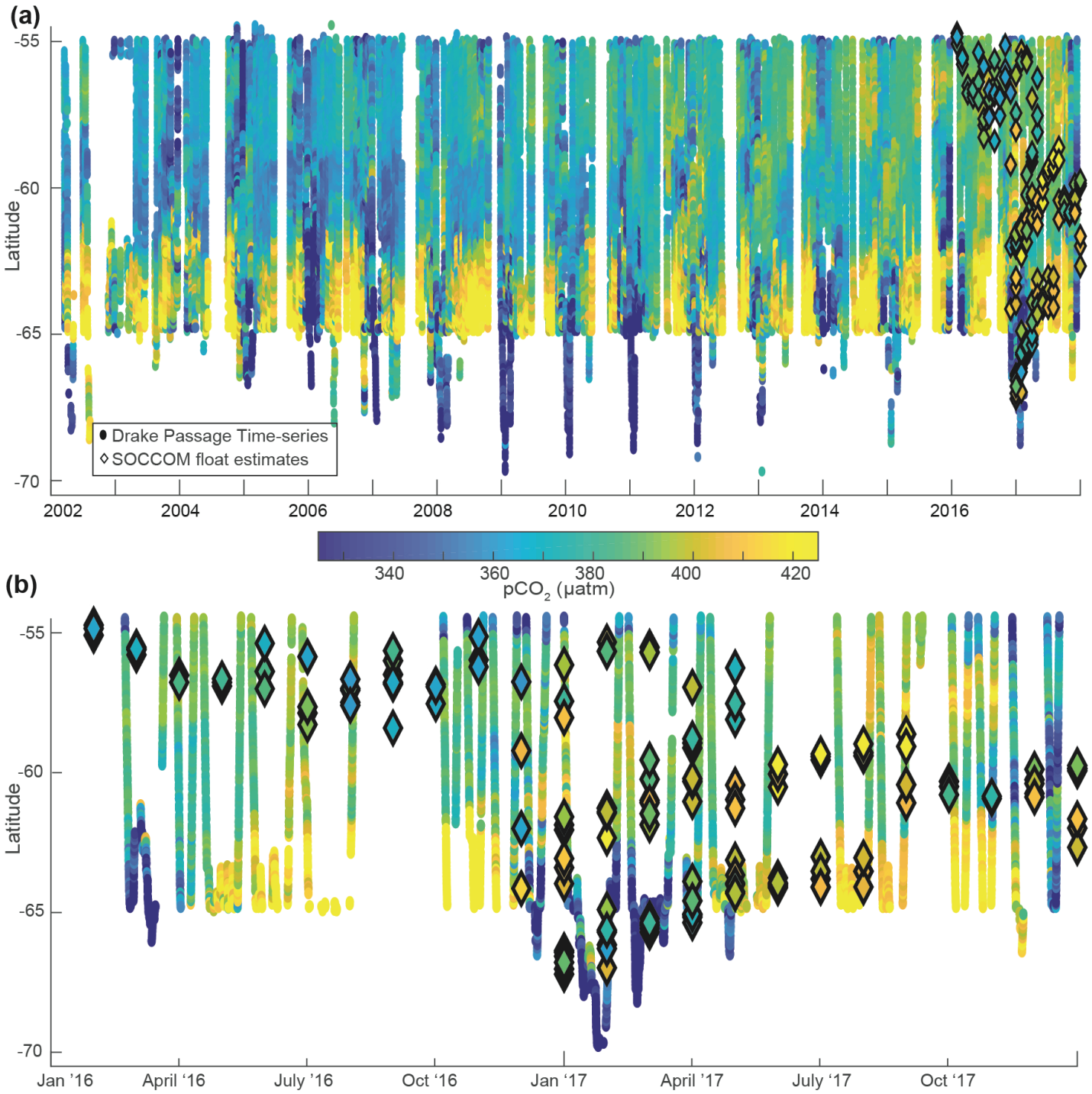
(a)
-55
-60
-65
-70
Latitude
Drake Passage Time-series
SOCCOM float estimates
2002
2004
2006
2008
2010
2012
2014
2016
340
360
380
400
420
pCO2 (µatm)
(b)
-55
-60
-65
-70
Latitude
Jan '16
April '16
July '16
Oct '16
Jan '17
April '17
July '17
Oct '17

Figure 9

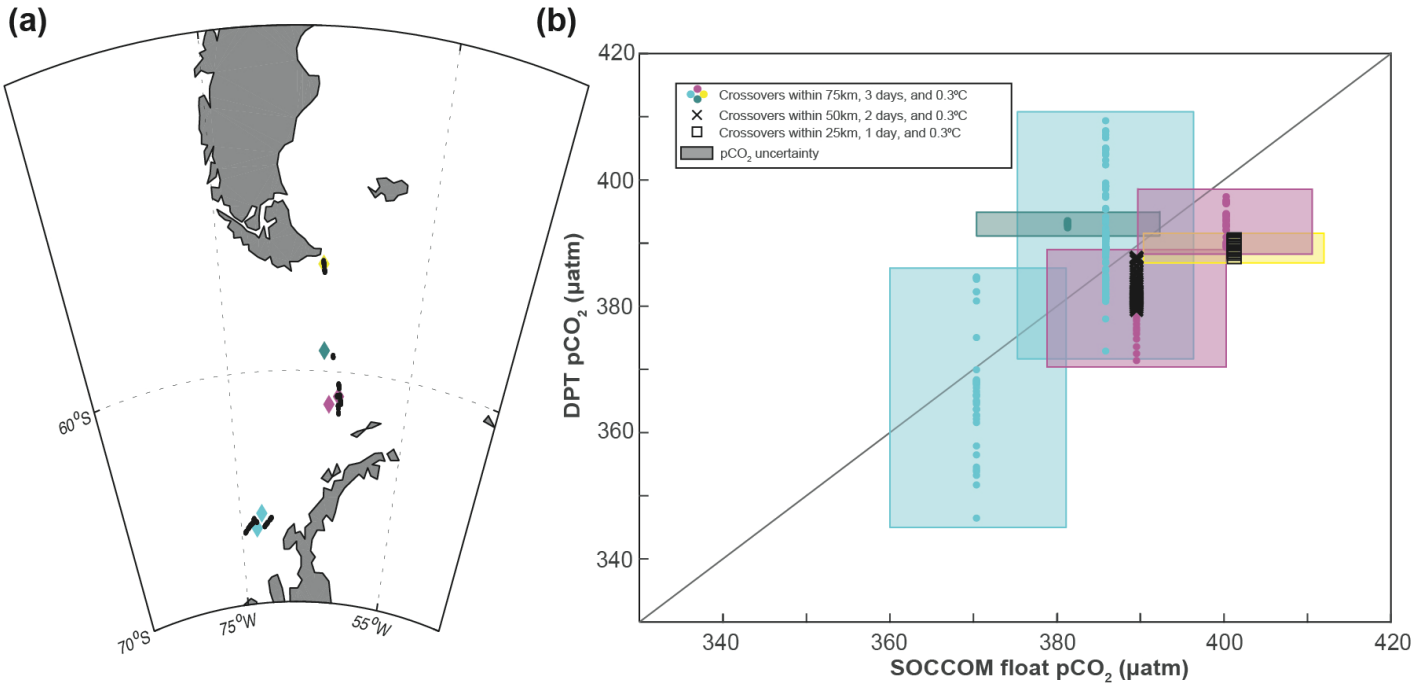
(a)
60°S
70°S
75°W
55°W
(b)
Crossovers within 75km, 3 days, and 0.3ºC
Crossovers within 50km, 2 days, and 0.3ºC
Crossovers within 25km, 1 day, and 0.3ºC
pCO2 uncertainty
DPT pCO2 (µatm)
SOCCOM float pCO2 (µatm)
340
360
380
400
420